SUPPLEMENTAL MATERIAL

Fine tuning of Sox17 and canonical Wnt coordinates the permeability properties of the blood-brain barrier

Monica Corada, Fabrizio Orsenigo, Ganesh Parameshwar Bhat, Lei Liu Conze, Ferruccio Breviario, Sara Isabel Cunha, Lena Claesson-Welsh, Galina V. Beznoussenko, Alexander A. Mironov, Marco Bacigaluppi, Gianvito Martino, Mara E. Pitulescu, Ralf H. Adams, Peetra Magnusson and Elisabetta Dejana

Expanded Methods

Mutant mice and inducible genetic modifications

All animal procedures were performed in accordance with the Institutional Animal Care and Use Committee, in compliance with the guidelines established in the Principles of Laboratory Animal Care (directive 86/609/EEC) and approved by the Italian Ministry of Health.

The following mouse strains were used: *Sox17*$^{flox/flox}$ [1]; β-*catenin*$^{flox(ex3)/flox(ex3)}$ [2]; Tg(BAT-LacZ) (The Jackson laboratory, stock 005317)[3]; *Dll4* $^{flox/flox}$[4]; *Rbpj*$^{flox/flox}$[5]; *Gt(ROSA)26-Sor*$^{tm1(Notch1)Dam/J}$ [6] and *Cdh5(PAC)*-Cre-ER^{T2} (Taconic Biosciences GmbH, 13073)[7].

The Sox17 conditional knock-out (Sox17^{iECKO}) and the endothelial-specific β-catenin gain-of-function (GOF) were generated as described previously[8, 9]. Sox17^{iECKO} mice were also interbred with Tg(BAT-LacZ) mice. For combined endothelial-cell-specific Sox17^{iECKO} and β-catenin GOF, β-catenin$^{flox(ex3)/flox(ex3)}$*/Cdh5(PAC)*-Cre-ER^{T2+} mice were interbred with *Sox17*$^{flox/flox}$*/Cdh5(PAC)*-Cre-ER^{T2+} mice. The resulting *Sox17*$^{flox/wt}$/β-catenin$^{flox(ex3)/wt}$*/Cdh5(PAC)*-Cre-ER^{T2+} mice were intercrossed with *Sox17*$^{flox/flox}$*/Cdh5(PAC)*-Cre-ER^{T2+} mice. Among the progeny, the following mice were selected for the experiments: *Sox17*$^{flox/flox}$/β-catenin$^{flox(ex3)/wt}$*/Cdh5(PAC)*-Cre-ER^{T2+}(Sox17^{iECKO}*/GOF*); *Sox17*$^{flox/flox}$/β-catenin$^{flox(ex3)/wt}$*/Cdh5(PAC)*-Cre-ER^{T2-} (wt); and *Sox17*$^{flox/flox}$/β-catenin$^{wt/wt}$*/Cdh5(PAC)*-Cre-ER^{T2+} (Sox17^{iECKO}).

To inactivate Dll4 and Rbpj in the postnatal endothelium, *Dll4* $^{flox/flox}$ and *Rbpj*$^{flox/flox}$ mice were interbred with *Cdh5(PAC)*-Cre-ER^{T2}.

To induce expression of active Notch, *Gt(ROSA)26-Sor*$^{tm1(Notch1)Dam/J}$ homozygous mice, carrying an inducible transgene for Notch1 intracellular domain overexpression (NICD), were interbred with *Cdh5(PAC)*-Cre-ER^{T2} mice.

C57BL/6 mice, 8-10 weeks old were purchased from Charles River Laboratories (Calco, Italy)

The conditional knock-in of td-Tomato-T2A-dnTcf4 (*dnTcf4*$^{flox(stop)/flox(stop)}$) in the *ROSA26* locus was generated by Taconic Biosciences GmbH (Cologne, Germany). In brief, the coding sequences of the reporter gene tdTomato and the dominant-negative form of Tcf4[10], linked by the T2A self-cleaving peptide, were cloned into a proprietary targeting vector downstream of the CAG promoter. A strong transcriptional stop cassette flanked by loxP sites was inserted between the promoter and the coding sequence, to prevent transcription in the absence of Cre activity. The targeting construct was fully sequenced and transfected into C57BL/6NTac embryonic stem cells equipped with a Flp recombinase-mediated cassette exchange landing platform in the Rosa26 locus. The insertion of the vector in the Rosa26 locus was mediated by Flp-directed recombination[11]. Targeted clones were identified by genomic PCR and validated by Southern blotting. Chimeras generated using the validated clones were bred with wt C57BL/6NTac females to obtain germline transmission. The *dnTcf4*$^{flox(stop)/flox(stop)}$ conditional knock-in mice were interbred with the *Cdh5(PAC)*-Cre-ER^{T2} transgenic line. *dnTcf4*$^{flox(stop)/wt}$*Cdh5(PAC)*-Cre-ER^{T2+} mice were interbred with *dnTcf4*$^{flox(stop)/flox(stop)}$ mice to generate litters containing *dnTcf4*$^{flox(stop)/flox(stop)}$*/Cdh5(PAC)*-Cre-ER^{T2+} (dnTcf4^{iECKI}) mice and control *dnTcf4*$^{flox(stop)/flox(stop)}$*/Cdh5(PAC)*-Cre-ER^{T2-} mice (wt). All of the mouse strains were backcrossed onto the C57BL/6J background for more than 12 generations.

Tamoxifen (T5648; Sigma-Aldrich) was dissolved in 10% ethanol-sunflower oil (10 mg/mL) and administered to the mice to induce Cre activity and genetic modifications. Mice were injected as described below. Pups were treated: (a) to inactivate Sox17, subcutaneously with 100 μg tamoxifen in the neck skin for

every pup of the litter on postnatal day 1 (P1); (b) to inactivate Dll4, pups were injected at P1 and P3 with 50 μg tamoxifen and analysed at P6; (c) to delete Rbpj, pups were injected every day, from P1 to P3 with 50 μg tamoxifen and analysed at P8; (d) to induce expression of NICD, pups were injected with 50 μg tamoxifen at P1 and P3 and analysed at P7. Pregnant females were intraperitoneally treated with two injections of 1 mg tamoxifen on days 11.5 and 13.5 post-coitum (pc). 6-week-old mice, were intraperitoneally treated with four injections of 1.5 mg tamoxifen once every other day, followed by 1 week prior to harvesting.

Pregnant females were defined following overnight mating, where they were examined the following morning for the presence of a vaginal plug; if present, this was counted as day 0.5 pc.

In all of the genetic experiments, the control mice (wt) refer to tamoxifen-injected mice that did not harbor the Cre transgene. Both males and females (in equal proportion) were used in this study.

Antibodies

The following antibodies were used for immunohistochemistry: anti-β-galactosidase (1:500, Abcam), isolectin-B4 (1:200, Vector Laboratories), anti-Sox17 (1:200, R&D Systems), anti-Podocalyxin (1:400, R&D Systems), anti-collagen IV (1:200, BioRad), anti-Ter119 (1:200, BD Biosciences), anti-PLVAP (1:100, BD Biosciences), anti-ERG (1:400, Abcam), and anti-Claudin-5 (1:100, FITC-conjugated; ThermoFisher Scientific), anti-Cingulin (1:500, ThermoFisher Scientific), anti-ZO-1 (1:200, ThermoFisher Scientific), anti-CD13 (1:200, R&D), anti-active Caspase 3 (1:100, Millipore). Alexa Fluor 488, 555 and 647 donkey secondary antibodies and streptavidin were from Jackson ImmunoResearch (1:400). Alexa Fluor 488 conjugated donkey anti-mouse was used to detect murine IgG (1:400, Jackson ImmunoResearch). For a detailed list of the antibodies used, please refer to Online Table II.

Tissue processing and immunohistochemistry

All immunostaining of both control and mutant samples was carried out simultaneously and under the same conditions. Tissues were prepared and processed for immunohistochemical analysis as described previously[8, 9, 12]. Briefly, hindbrains from embryos of embryonic days (E) 10.5, 12.5, 14, and 17 were dissected out in cold phosphate-buffered saline (PBS), fixed in 4% paraformaldehyde (PFA) overnight at 4 °C, and stained as whole-mounts, as described previously[13]. After blocking and permeabilization in PBS containing 5% donkey serum, 1% bovine serum albumin (BSA) and 0.3% Triton X-100, for 2 h at room temperature, the hindbrains were incubated overnight with primary antibodies diluted in blocking/permeabilization solution. Following washes with 0.3% Triton X-100 in PBS, the Alexa-Fluor-coupled secondary antibodies (Jackson ImmunoResearch) were added, and incubated overnight at 4 °C. The next day, the hindbrains were washed with 0.3% Triton X-100 in PBS and flat-mounted using Vectashield containing DAPI (H-1200; Vector).

Brains from embryos (E15.5) and early postnatal pups (P5, P9) were harvested and immersion fixed overnight in 4% PFA at 4 °C. After several washes with PBS, the fixed brains were cryoprotected and processed for cryo-sectioning.

To harvest brains from adult mice, the mice were anesthesized by intraperitoneal injection of Avertin (T48402; Sigma) (20 mg/kg), and perfused with 1% PFA in PBS. The brains were carefully dissected out from the skull and post-fixed overnight by immersion in 3% PFA at 4 °C. The next day they were washed in PBS and processed for sectioning.

For vibratome (1000 Plus; The Vibratome Company) sections, the brains were embedded in 3% low-melting-point agarose, sectioned (100 μm), and immunostained. Coronal and sagittal vibratome sections were incubated in blocking/permeabilization solution (1% BSA, 0.3% Triton X-100, in PBS) overnight at 4 °C. This was followed by incubation in the primary antibody solution, and subsequently in the secondary antibody solution, both overnight at 4 °C. Sections were mounted in Vectashield that contained DAPI (H-1200; Vector).

For cryosectioning, fixed brains were cryo-protected in 30% sucrose overnight at 4 °C and embedded in Killik embedding medium (059801; BioOptica). Sections (20 μm) were cut using a cryostat (Leica), then mounted on positively charged glass slides and stained as described above.

To analyze the retina vascular phenotype, the eyes (P9) were fixed in 3% PFA in PBS for 2 h at 4 °C, and then dissected as described previously[9]. Whole-mount retinas were incubated at 4 °C overnight in primary antibody diluted in PBSTC buffer (0.5% Triton X-100, 0.1 mM $CaCl_2$, in PBS) containing 5% donkey serum, followed by the secondary antibody staining, overnight at 4 °C, using suitable species-specific Alexa Fluor-

coupled antibodies (Jackson ImmunoResearch). These samples were then flat-mounted on glass microscope slides with Prolong Gold antifade reagent (P36930; ThermoFisher Scientific). For immunofluorescence analysis, negative controls using isotype matched normal IgG were done to check for antibody specificity.

VEGF injections

The recombinant adeno-associated virus (AAV) vectors of serotype 9 were kindly provided by Prof. Kari Alitalo, University of Helsinki[14]. Here, 3×10^9 AAV9 particles encoding human VEGF were injected in deeply anesthetized (intraperitoneal injection of Avertin, 20mg/Kg) 7-8-week-old mice (*Sox17*^{iECKO}, wt) using a stereotaxic instrument and the following coordinates: 1 mm anterior to the bregma; 1.5 mm right of the midline; 2.7 mm ventral to the surface of the skull. After surgery, carprofen (5mg/kg subcutaneously) was given as a pain reliever and mice were placed in a recovery rack. At 48 h after injection, the mice were deeply anesthetized and perfused as described above. The brains were processed for vibratome sectioning.

Cadaverine permeability assay

Lysine-fixable, Alexa Fluor-555 conjugated cadaverine (ThermoFisher Scientific) (25 mg/kg) was injected intravenously into the tail vein of adult mice, and intraperitoneally in the pups, 2 h prior to sacrifice. The animals were anesthesized by intraperitoneal injection of Avertin (T48402; Sigma) (20 mg/kg), and perfused as above. The brains from 4 animals per group were dissected out and fixed for up to 8 h by immersion in 4% PFA at 4 ℃, then washed in PBS, and prepared for vibratome sectioning. Brains were fully sectioned. Representative sections (rostral to caudal) are shown in Online Figure IIA.

Treatment with GSK-3β inhibitor

For the *in vivo* inhibition of GSK-3β, tamoxifen was injected at P1, and then 6-BIO ((2'*Z*,3'*E*)-6-bromoindirubin-3'-acetoxime, BIO-Acetoxime; Calbiochem, 361551) and as control MeBIO (1-methyl-BIO; Calbiochem, 361556), at 5 mg/kg/day injected intraperitoneally from P5 to P7. Pups at postnatal day 8 (P8), were anesthetized and perfused as described above. The brains and retina were processed for immunohistochemical analysis as described above.

Treatment with DAPT

Notch signaling was inhibited in the pups by subcutaneous injection with 100 mg/ kg DAPT (Alexis Bioscience) in 10% ethanol and 90% corn oil or vehicle only, from P4 to P6 and analysed at P7.

Mouse Ischemic Stroke model

Mice underwent 45 minutes left Middle Cerebral Artery Occlusion (MCAO), as described[15]. Briefly, animals were anesthetized with 1-1.5% isofluorane (Merial, Assago, Italy) in 30% O_2. Temperature was maintained between 36.5 and 37.0°C and Laser Doppler flow (LDF) was monitored. Focal cerebral ischemia of the middle cerebral artery was induced with a silicon-coated (Doccol, Sharon, MA, USA, 702034PK5Re) 7-0 nylon filament. Following 45 min of MCAO, reperfusion was induced by withdrawing the filament. Wounds were carefully sutured, anesthesia was discontinued and mice were put back in their cages to allow recovery. Mice were sacrificed and used for longitudinal gene expression analysis or brain tissue pathology at 0, 3, 6, 13 and 33 days (as indicated in specific figure panels) post ischemia, as described below.

Post ischemia behavioral analyses. The modified Neurological Severity Score (mNSS) - a motor and coordination test battery assessing the severity of the neurological deficits on a graded scale ranging from 0 to 14, where 0 represents normal function and 14 maximal deficits – was evaluated at baseline, at each day after stroke as previously described[15]. Behavioral tests were performed by a researcher blinded to the genotype of the mice during the light phase of the circadian cycle beginning 4 hours after lights on.

Analysis of infarct size. For the measurement of the ischemic lesion volume, coronal 20 μm-thick coronal cryostat sections were prepared from 2 mm rostral to 4 mm caudal to the bregma. One systematic random series of sections per mouse was stained for cresyl violet (Sigma), digitalized and analysed with Image J (NIH, USA) image analysis system. The lesion area was measured for each reference level by the '*indirect method*', as previously described[15]. For the representative 3D volume rendering images a representative brain stained by cresyl violet was traced using the assistance of the Stereo Investigator v 3.0 software (MicroBrightField, Inc.,

Colchester, VT) and a personal computer running the software connected to a color video camera mounted on a Leica microscope as described [16, 17].

Tissue pathology. At the indicated reperfusion times, animals were deeply anaesthetized and transcardially perfused with 25mL of saline phosphate buffer (PBS 0.1 M, pH 7.2) with EDTA, followed by 25mL of 4% PFA. Brains were carefully dissected, postfixed overnight, cryoprotected in sucrose and embedded in tissue-freezing medium for cryostat sectioning. Frozen brains were cut into 20- 50 µm thick coronal cryostat sections.

Gene expression analysis. Animals used for gene expression studies were sacrificed at the indicated reperfusion times by transcardiac perfusion with 0.1 M PBS preceded by induction of deep anaesthesia. Brains were rapidly removed and dissected on an ice block. A representative coronal brain slice including both the striatum and cortex was harvested from the level 2 mm rostral to 2 mm caudal to bregma. The two hemispheres were cutted along the midline, separately processed and total RNA isolated using the RNeasy Lipid Tissue kit (#74804; Qiagen) according to the manufacturer's instructions, including DNase digestion. cDNA was synthesized from 5 µg of total RNA using the Ready-to-Go You Prime First Strand Beads (#27-9264-01; GE Healthcare) and Random Hexamer (New England Biolabs, #S1230S) according to the manufacturer's instructions. Two- hundred ng of cDNA were used for RT-qPCR using pre-designed Taqman Gene Expression Assays (Applied Biosystems). RT-qPCRs were performed using an ABI Prism™ 7700 Sequence Detection System (Applied Biosystems) according to manufacturer's protocol and using specific assays (Sox17, Mm00488363_m1). Data were collected with instrument spectral compensations by the Applied Biosystems SDS 1.9.1 software and analysed using the threshold cycle (C_T) relative quantification method to the housekeeping gene Gapdh as previously described[15].

Statistical analysis. Stroke lesion volume and edema between treatment groups was compared using Mann-Whitney test as indicated in the figure legend. The significance level was established at $p \leq 0.05$. Behavioral tests were evaluated by means of repeated measurement analysis of variance (two-way ANOVA). Whenever a treatment by time interaction or treatment effect was present at the 0.05 level, a post-hoc analysis was done by Bonferroni post-hoc test. Gene expression levels were compared using one-way ANOVA, followed by Bonferroni post-hoc test. Survival curves were compared using the Log-rank (Mantel-Cox) Test. A standard software package (GraphPad Prism, version 5.00f) was used.

3D reconstruction. For the representative 3D volume rendering images a representative brain stained by cresyl violet was traced using the assistance of the Stereo Investigator v 3.0 software (MicroBrightField, Inc., Colchester, VT) and a personal computer running the software connected to a color video camera mounted on a Leica microscope as described[16, 17].

Electron Microscopy

Basic electron microscopic (EM) examination and immune EM analysis was performed exactly as described earlier[18, 19]. Procedure of tissue block preparation for EM analysis was the same as described before[20].

Image acquisition, processing and analysis

Confocal microscopy was performed (TCS SP2, SP5 or SP8 confocal microscopes; Leica). For image analysis Fiji software (open source; htpp://fiji.sc/) was used.

The figures were assembled and processed using Adobe Photoshop and Adobe Illustrator. The only adjustments used in the preparation of the figures were for brightness and contrast. For comparison purposes, different sample images of the same antigen were acquired under constant acquisition settings.

a) Quantification of β-gal and Sox17 was done as follow. For each confocal stack acquired, Isolectin B4 (or Podocalyxin) was used to create a binary mask of the vascular network. Both Sox17 and β-gal stacks were then multiplied by the corresponding binary mask to isolate ECs specific stacks preserving pixel intensity value. Lastly, Sox17/β-gal double positive nuclei were identified by applying the Colocalization Highlighter plugin of ImageJ to the ECs filtered stacks. Sox17, β-gal or double positive nuclei were then counted using the 3D object counter plugin[21] for ImageJ.

b) IgG intensity was measured as follow unless differently specified below. Each brain sagittal section was acquired with 10x microscopic lens. Then, using ImageJ, 6 regions of interest (ROI) were defined (3 in the cortex and 1 each in the striatum, the thalamus and the cerebellum). Mean intensity value of each ROI was then measured. The size and the relative position of the ROIs were kept constant within every comparison. The ROI

size for striatum, thalamus and cerebellum were defined to roughly cover the 80% of the region area. Three or more sections for each sample were used for quantification.
IgG intensity in embryonic brain was measured as the percentage of the section area positive to IgG (Threshold 78). This quantification method was preferred to the ROI described above because the uneven distribution of IgG signal within the sections. Three or more sections for each sample were used for quantification.
IgG intensity in the Stroke experiment was measured as above with the exceptions that ROIs were defined within the infarct region.
c) Quantification of hemorrhages, based on Ter119/Podocalyxin or Ter119/Collagen IV staining, and was done as follow. Slides were observed under fluorescence microscope following a "line-scanning" like pattern. Hemorrhagic spots were manually counted during the observation and expressed as the ratio of the number of spots counted vs the number of sections observed. Three or more sections for each sample were used for quantification.
d) To assess Cadaverine leakage, the mean pixel intensity value was measured for each microscopic field acquired. Three or more sections for each sample were used for quantification.
e) PLAVP, ZO-1, Cingulin and Claudin-5 staining were quantified as follow. For each confocal stack acquired, Podocalyxin was used to create a binary mask of the vascular network. Then, for each antigen, stacks were multiplied by the corresponding binary mask to isolate ECs specific stacks preserving pixel intensity value. Pixels mean intensity value was then measured on the filtered stacks.
f) Sox17 staining was quantified as follow. For each confocal stack acquired, ERG staining was used to create a binary mask of ECs nuclei. Then, Sox17 stacks were multiplied by the corresponding binary mask to isolate ECs specific nuclear staining preserving pixel intensity value. Pixels mean intensity value was then measured on the filtered stacks.
g) Quantification of β-gal positive nuclei was done by two distinct operators. The first operator acquired the confocal stacks, while the second operator manually counted β-gal and ERG positive cells in a blind test. Cell counting was adjuvated by the cell counter plugin of ImageJ. Results were then expressed as percentage of β-gal vs ERG positive cells.

Purification of brain ECs

Brains were enzymatically digested in combination with gentleMACS Octo Dissociator (Miltenyi Biotech), using Neural Tissue Dissociation kits (P) (130-092-628; Miltenyi Biotech) for embryos at E15.5 and pups at P5, and Adult Brain Dissociation kits (130-107-677; Miltenyi Biotech) for pups at P9 and adults. After dissociation, myelin cell debris and erythrocytes were removed according to the manufacturer protocol. ECs were enriched by depletion of CD45-positive cells with CD45 MicroBeads (30-052-301; Miltenyi Biotech), followed by positive selection using CD31 MicroBeads (30-097-418; Miltenyi Biotech). The final cell pellets were washed with PBS and processed for total RNA extraction. Total RNA was isolated using Maxwell RSC simplyRNA cells and tissue kits (AS1390, Promega), according to the manufacturer protocol. cDNA synthesis and RT-qPCR analysis were carried out as described previously[8, 9].

RNA-Seq

For each timepoint, the RNA-Seq was performed on three indipendent biological replicates.
Libraries for RNA sequencing were prepared following the manufacturer protocols for transcriptome sequencing with an Ion Proton sequencer (ThermoFisher Scientific). Briefly, 1 μg total RNA was poly-A selected using Dynabeads mRNA Direct Micro Purification kits (61021; ThermoFisher Scientific), according to manufacturer protocol. About 50 ng poly-A RNA were used to prepare strand-specific barcoded RNA libraries, with Ion Total RNA-Seq kits v2.0 (4475936; ThermoFisher Scientific). Briefly poly-A RNAs were fragmented with RNAse III and purified with Nucleic Acid Binding Beads. After purification, the fragmented poly-A RNAs were hybridized and ligated with Ion Adaptor, and subsequently reverse transcribed for cDNA preparation. The cDNAs were amplified with Ion Torrent barcode primer and purified with Nucleic Acid Binding Beads. The final libraries were quantified on a fluorimeter (Qubit) with HS DNA (ThermoFisher Scientific), and checked for size on an Agilent Bioanalyzer with HS DNA kits (Agilent).

Four barcoded libraries were pooled together on an equimolar basis to the final concentration of 11 pM, and clonally amplified using Ion Proton Hi-QTemplate kits (ThermoFisher Scientific). With an IonOneTouch 2

instrument (ThermoFisher Scientific). After emulsion PCR, DNA positive Ion Sphere Particles (ISPs) were recovered and enriched according to standard protocols, using an IonOneTouch ES instrument (ThermoFisher Scientific). A sequencing primer was annealed to DNA-positive ISPs and the sequencing polymerase bound, prior to loading of ISPs into Ion P1 sequencing chips. Sequencing of the samples was carried out according to the Ion Proton Hi-Q Sequencing kit protocol on and Ion Proton instrument.

RNA-Seq data analysis

Each sample received ~20 to 25 million of single-end reads. Trim Galore (http://www.bioinformatics.babraham.ac.uk/projects/trim_galore/) was used for quality/adapter trimming of the raw reads. In addition, 5 nucleotides from both 5' and 3' end of the reads were clipped to remove unwanted bias. The trimmed reads were aligned to the mm10 mouse reference with >80% unique mapping rate using STAR[22] (version 2.5.3a), and HTSeq-count[23] (version 0.9.1) was used to quantify gene expression by read count. For GO annotation of the genes, BiomaRt[24], an R package on Bioconductor, was used.

We assessed the quality of RNA-Seq data by checking the distribution of gene expression levels (log transformed TPM). It follows Poisson distribution in all the samples and replicates, which fits with the assumption of the statistical model used by the downstream programs such as R package DESeq2 to calculate differentially expressed genes. To visualize the overall effect of experimental covariates and batch effects, we showed sample to sample distance in principal component (PCA) plot. The PCA plot indicates that the variation between the biological replicates in our RNA-Seq data is very low (Online Figure XII).

Time course analysis: The read counts were normalized by transcript per million (TPM) and only genes with TPM≥1 in all samples were used as input in Next-maSigPro[25], an R package on Bioconductor, for the time course analysis. Next-maSigPro uses generalized linear models (GLM) to model RNA-seq count data. This is achieved by fitting to a negative binomial distribution followed by a polynomial regression. The p-value below 0.05 was set as cut-off for identifying differentially expressed genes in this step. In the second step of maSigPro, the goodness of fit, R^2, of each optimized gene model is computed. $R^2 > 0.6$ is used for selecting genes with clear expression trends. Finally, the significant genes ($p<0.05$ and $R^2 > 0.6$) were clustered using k-mean clustering method, the number of clusters was set to 6.

Pairwise analysis: Genes with one or more read counts in at least one sample were used as input in DESeq2[26], an R package on Bioconductor, for the pairwise differential expression analysis. |Log2FC|≥0.4 and the adjusted *p*-value≤0.05 are the thresholds for identifying significantly differentially expressed genes (DEGs).

We compared $Sox17^{iECKO}$ and wt newborn pups at P5 and P9. We analyzed gene expression of E15.5 embryos and adult mice separately since the time after tamoxifen injection was different.

Time course analysis: The read counts were converted to transcript per million (TPM) and only genes with TPM≥1 in all samples were used as input in Next-maSigPro[25], an R package on Bioconductor, for the time course analysis. The p-value below 0.05 was set as cut-off for identifying differentially expressed genes. Using a stringency R^2 value of 0.6, a subset of differentially expressed genes were clustered into 6 groups based on their expression pattern over time.

GO enrichment analysis: To identify enriched functional groups in DEGs from both pairwise and time course analysis, topGO[27], an R package on Bioconductor, was used. GO terms were considered significantly enriched in the data sets, if the *p*-value from Fisher's exact test with *weight01* algorithm is below 0.05. The thresholds $p<0.05$, annotated ≥ 40, significant ≥ 3 and significant/expected ≥ 2.5 are used for selecting most significant over-represented GO terms for visualizing in Figure 5C.

The authors declare that all data supporting the findings of this study are available within the article and its supplementary information files or from the corresponding author upon reasonable request. The RNA sequencing data have been deposited in the Gene Expression Omnibus (GEO) database under accession code GSE122564. Data can also be explored at https://edgroup.shinyapps.io/sox17_bbb/ .

Cell culture and PLA

Brain ECs (iBMEC) were isolated from $Sox17^{flox/flox}$ pups (P4) as described above. The cells were then immortalized in culture through retroviral expression of polyoma middle T antigen, as described previously[28], and Sox17 was inactivated by treating the cultured ECs with TAT-Cre recombinase[29].

Sox17-null ECs, were lentivirally transduced with GFP or *Sox17* cDNAs, subcloned into the lentiviral plasmid pRRLsin.PPTs.hCMV.GFPwpre under the transcription of CMV promoter[30].

Brain ECs were grown in MCDB-131 (ThermoFisher Scientific) with 20% fetal bovine serum (HyClone), heparin 100 μg/mL (H3149; Sigma), and ECs growth supplement at 50 μg/mL (E2759; Sigma)[9].

For *in situ* PLA experiments, iBMEC (passage 15 to 17) were seeded at the density of 50,000/cm^2 onto glass coverslips and grown to confluence. ECs confluent monolayer was serum starved (MCDB-131, 1% BSA) overnight, and then incubated with 50 ng/ml Wnt 3a (R&D) for 2 h. Cells were fixed with 1% PFA in triethanolamine, pH 7.5, containing 0.1% Triton X-100 and 0.1% NP-40.

Fixed cells were processed following the manufacturer instructions (Duolink® In Situ Orange Starter Kit Goat/Rabbit, DUO92106, Sigma). The primary antibodies used were: goat anti Sox17 (1:100, R&D) and rabbit anti β-catenin (1:200, Sigma), followed by incubation with anti-goat and anti-rabbit PLA probes.
Confocal stacks were acquired using 63x oil immersion lens, under constant acquisition settings. Quantification of PLA nuclear spot was done as follow. For each confocal stack acquired, DAPI staining was either used to create a binary mask of ECs nuclei and to count the number of cells in each field. Then, PLA stacks were multiplied by the corresponding binary mask to isolate nuclear spots, which was counted using the Analyze particle plugin of ImageJ. Results are expressed as average number of PLA spots per cell.

Statistical analysis

Beside stroke experiments (see above), statistical significance was assessed as follow. Normality of datasets was assessed by Shapiro-Wilk normality test. For datasets presenting normal distribution, two-tailed t-test assuming unequal variance (for pairwise comparison) or one-way ANOVA followed by Bonferroni's or Tukey's post-hoc test (for multiple comparison) was used. Non-parametric (Mann-Whitney test) was applied to datasets which did not show normal distribution. Whenever applicable, the applied statistical test is specified in the figure legend. A standard software package (GraphPad Prism, version 7.00d) was used.

Online Table II. List of antibodies used.

Primary Antibodies

Antibody	*Brand*	*Catalog number*	*Dilution*
Chicken polyclonal anti-β-galactosidase	Abcam	Cat # ab9361	1:500
Biotynilated Griffonia Simplicifolia Lectin I (GSL I) isolectin B4	Vector Laboratories	Cat # B1205	1:200
Goat polyclonal anti-Sox17	R&D	Cat # AF1924	1:200
Goat polyclonal anti-Podocalyxin	R&D	Cat # AF1556	1:400
Rabbit polyclonal anti-Collagen IV	BioRad	Cat # 2150-1470	1:200
Rat monoclonal anti-Ter119	BD Biosciences	Cat # 553671	1:200
Rat monoclonal anti-PLVAP/MECA-32	BD Biosciences	Cat # 553849	1:100
Rabbit monoclonal-anti ERG	Abcam	Cat # ab92513	1:400
Mouse monoclonal anti-Claudin-5, Alexa 488 conjugate	Thermo Fisher Scientific	Cat # 352588	1:100
Rabbit polyclonal anti-cingulin	Thermo Fisher Scientific	Cat # 364401	1:500
Rabbit polyclonal anti-β-catenin	Sigma	Cat # PLA0230	1:200
Rat monoclonal anti-CD31	BD Biosciences	Cat # 550274	1:200
Rabbit polyclona anti-ZO-1	Thermo Fisher Scientific	Cat # 617300	1:200
Goat polyclonal anti-CD13	R&D	Cat # AF2335	1:200
Cleaved Caspase3	Millipore	Cat # Ab3623	1:100

Secondary Antibodies

Antibody	*Brand*	*Catalog number*	*Dilution*
Donkey polyclonal anti-goat IgG (H+L), affinity-purified secondary antibody, Alexa 488, Cyanine Cy™ 3 and 647 conjugates	Jackson ImmunoResearch	Cat #s: 705-545-147; 705-165-147; 705-605-147	1:400
Donkey polyclonal anti-rabbit IgG (H+L), affinity-purified secondary antibody, Alexa 488, Cyanine Cy™ 3 and 647	Jackson ImmunoResearch	Cat #s: 711-545-152; 711-165-152; 711-605-152	1:400
Donkey polyclonal anti-rat IgG (H+L), affinity-purified secondary antibody, Alexa 488, Cyanine Cy™ 3 and 647 conjugates	Jackson ImmunoResearch	Cat #s: 712-545-153; 712-165-153; 712-175-153	1:400
Donkey polyclonal anti-mouse IgG (H+L), affinity-purified secondary antibody, Alexa 488, Cyanine Cy™ 3 and 647 conjugates	Jackson ImmunoResearch	Cat #s: 715-545-151; 715-165-151; 715-605-151	1:400
Donkey polyclonal anti-chicken IgG (H+L), affinity-purified secondary antibody, Alexa 488 and Cyanine Cy™ 3 conjugates	Jackson ImmunoResearch	Cat #s: 703-545-155; 703-165-155	1:400
Streptavidin Alexa 488, Cyanine Cy™ 3 and 647 conjugates	Jackson ImmunoResearch	Cat #s: 016-540-084; 016-160-084; 016-600-084	1:400

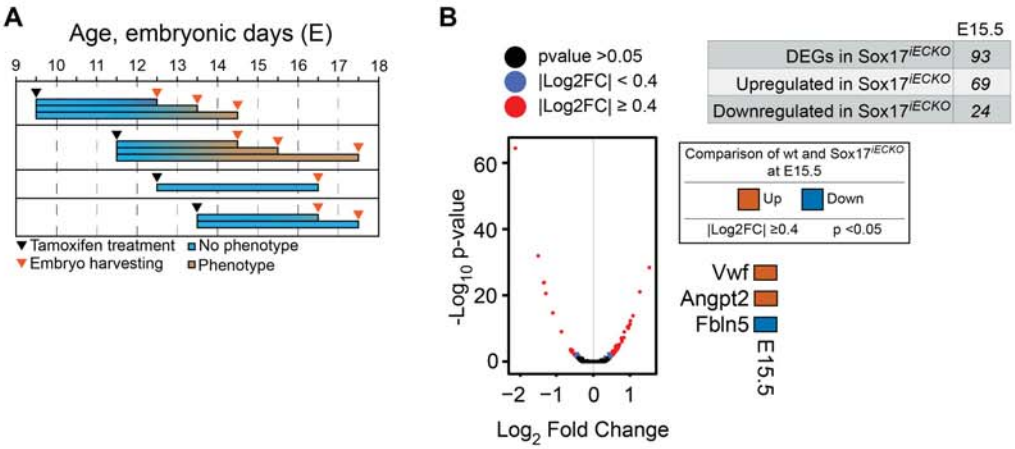

Online Figure I. Endothelial Sox17 inactivation in embryos

(A) Temporal analysis of the macroscopic appearance of the embryonic phenotypes. The severity of the phenotype following Sox17 inactivation depends on the developmental stage at which tamoxifen is administered, and on the time between Sox17 inactivation and embryo collection.

(B) Differential gene expression between wt and Sox17^{iECKO} brain ECs at E15.5. Volcano plots are used to display the magnitude (Log2 fold change) of the differential expression between wt and Sox17^{iECKO} at E15.5. Each dot represents one gene that has detectable expression both in wt and Sox17^{iECKO} cells. Black dots represent genes that are not differentially expressed significantly (adjusted p>0.05). Significantly DEGs (adjusted p≤0.05) are colored either in red (|Log2FC|≥0.4) or in blue (|Log2FC|<0.4). The number of DEGs in Sox17^{iECKO} are reported in the table on top of the Volcano plots. Among the list of DEGs shown in Figure 6, up (orange) or down (blue) some relevant examples of the genes regulated in Sox17^{iECKO} embryos are reported next to the Volcano plot. The overall number of Sox17 regulated genes at this time of development was relatively small.

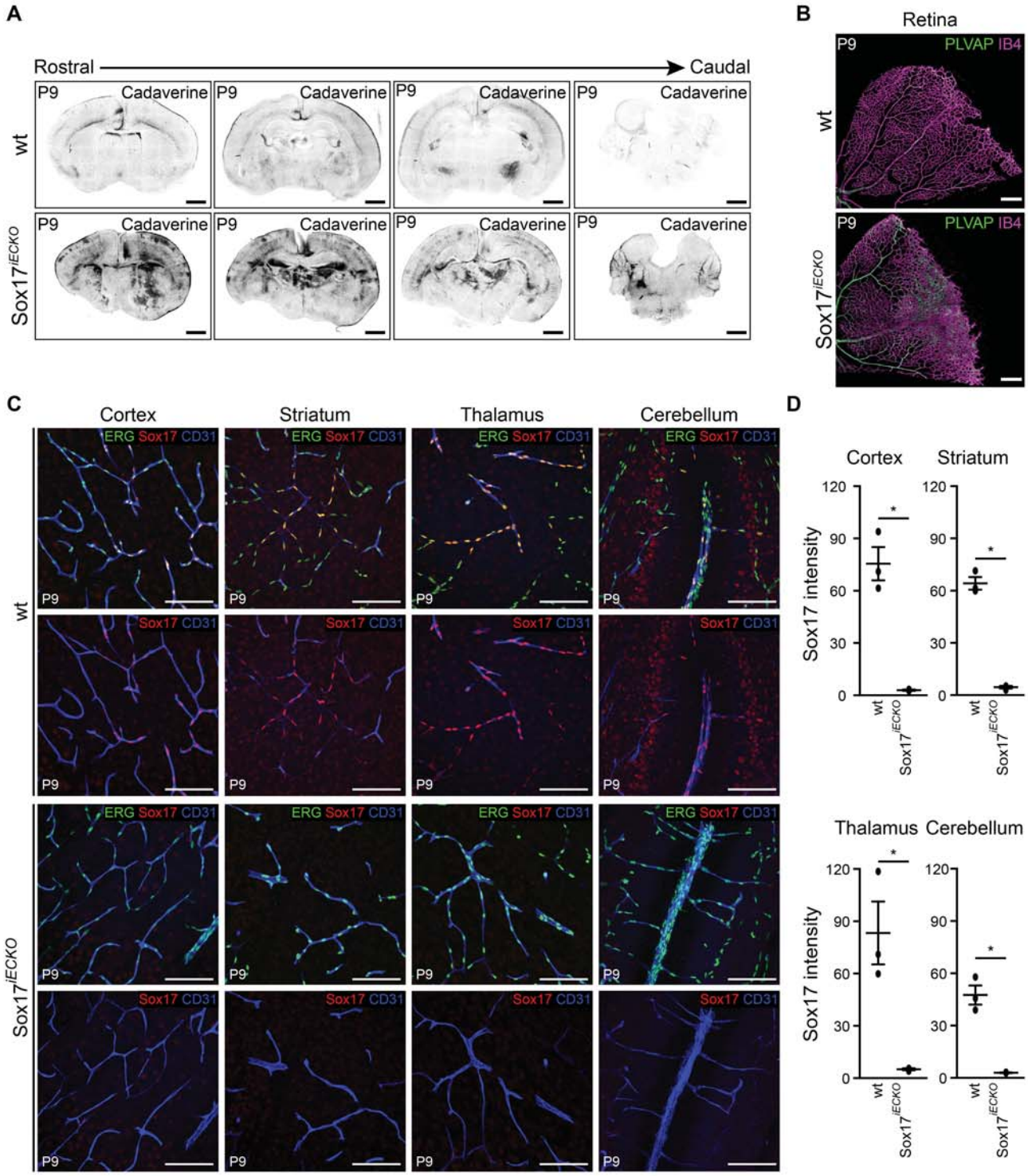

Online Figure II. Endothelial Sox17 inactivation in postnatal pups

(A) Representative confocal images of wt and Sox17^{iECKO} pup brain coronal sections (vibratome). The increased cadaverine leakage observed in Sox17^{iECKO} pups was present in all of the regions examined, which suggests that the effects of Sox17 inactivation are common to different types of vessels.

(B) Confocal images of PLVAP (green) and isolectinB4 (IB4, in magenta) in whole-mount retina of wt and Sox17^{iECKO} pups. PLVAP expression was increased in Sox17^{iECKO} mice (see also Figure 3F-G). Scale bar: 200 μm.

(C) Confocal analysis of Sox17 (red) downregulation in the vessels of Sox17^{iECKO} pup brains. Effective downregulation was observed in all the regions analyzed. Vessels are identified by CD31 (blue) and ECs nuclei

by ERG (green) labeling. Scale bar: 100 μm.
(D) Quantification of nuclear Sox17 expression in the the vasculature of the four brain regions analyzed, see methods for details. Data are represented as mean ± SEM (n=3 wt and 3 Sox17^{iECKO}, *p <0.01, two-tailed t-test assuming unequal variance).

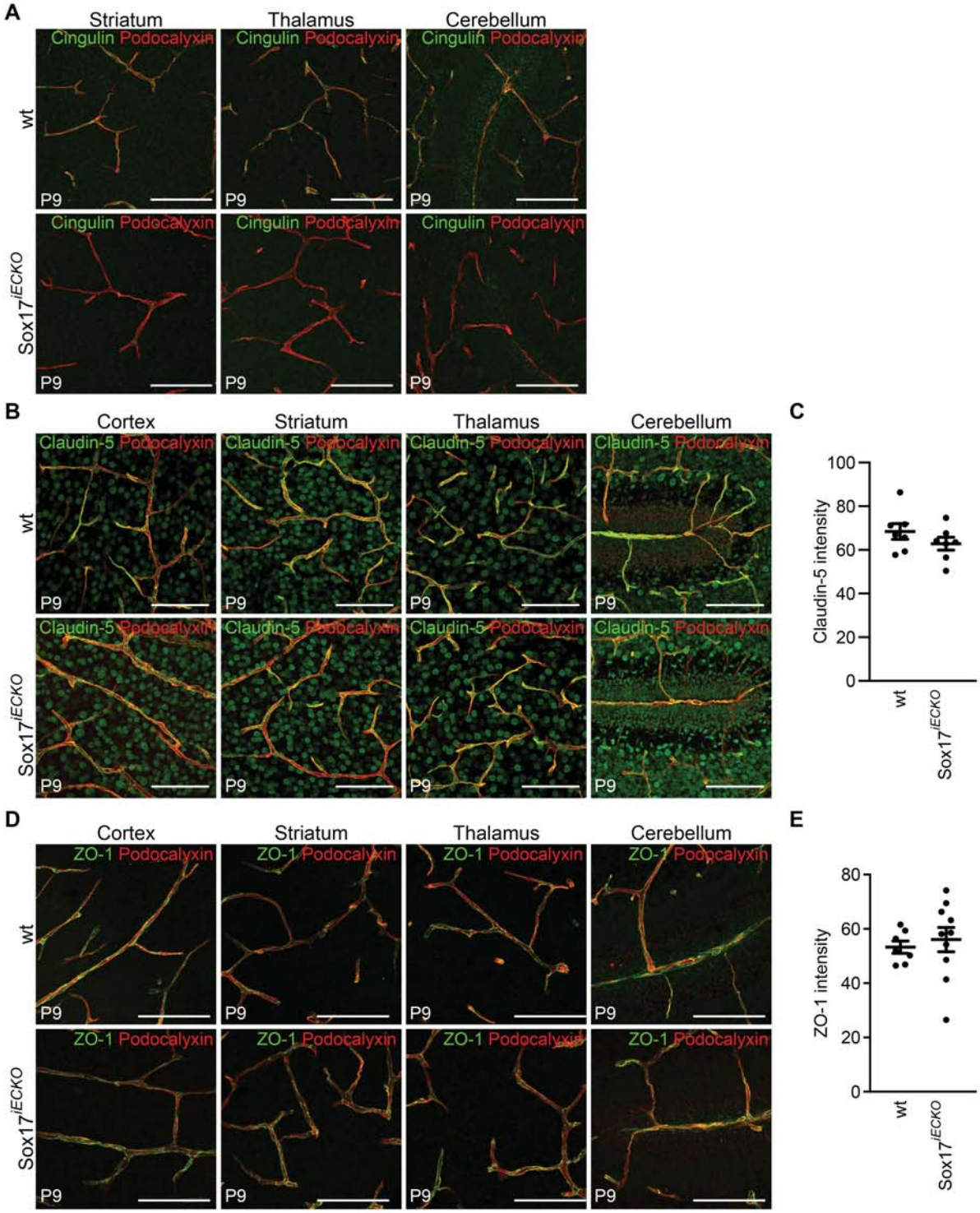

Online Figure III. Distribution of tight junction associated proteins in Sox17^{iECKO} endothelial cells

(A) Confocal analysis of Cingulin (green) and Podocalyxin (red) in different regions of wt and Sox17^{iECKO} pup brains (see Figure 3 for the Cortex and the quantification). Cingulin staining was significantly reduced in Sox17^{iECKO} vessels (lower panels). Scale bar: 100 μm.

(B-C) Confocal analysis and quantification of Claudin-5 (green) in different regions of wt and Sox17^{iECKO} pup brains. Vessels are labelled with Podocalyxin (red). Scale bar: 100 μm. Data in (C) are represented as mean ± SEM. (n=3 wt and 3 Sox17^{iECKO}).

(D-E) Confocal analysis and quantification of ZO-1 (green) in different regions of wt and Sox17^{iECKO} pup brains. Vessels are labelled with Podocalyxin (red). Scale bar: 100 μm. Data in (C) are represented as mean ± SEM. (n=3 wt and 3 Sox17^{iECKO}).

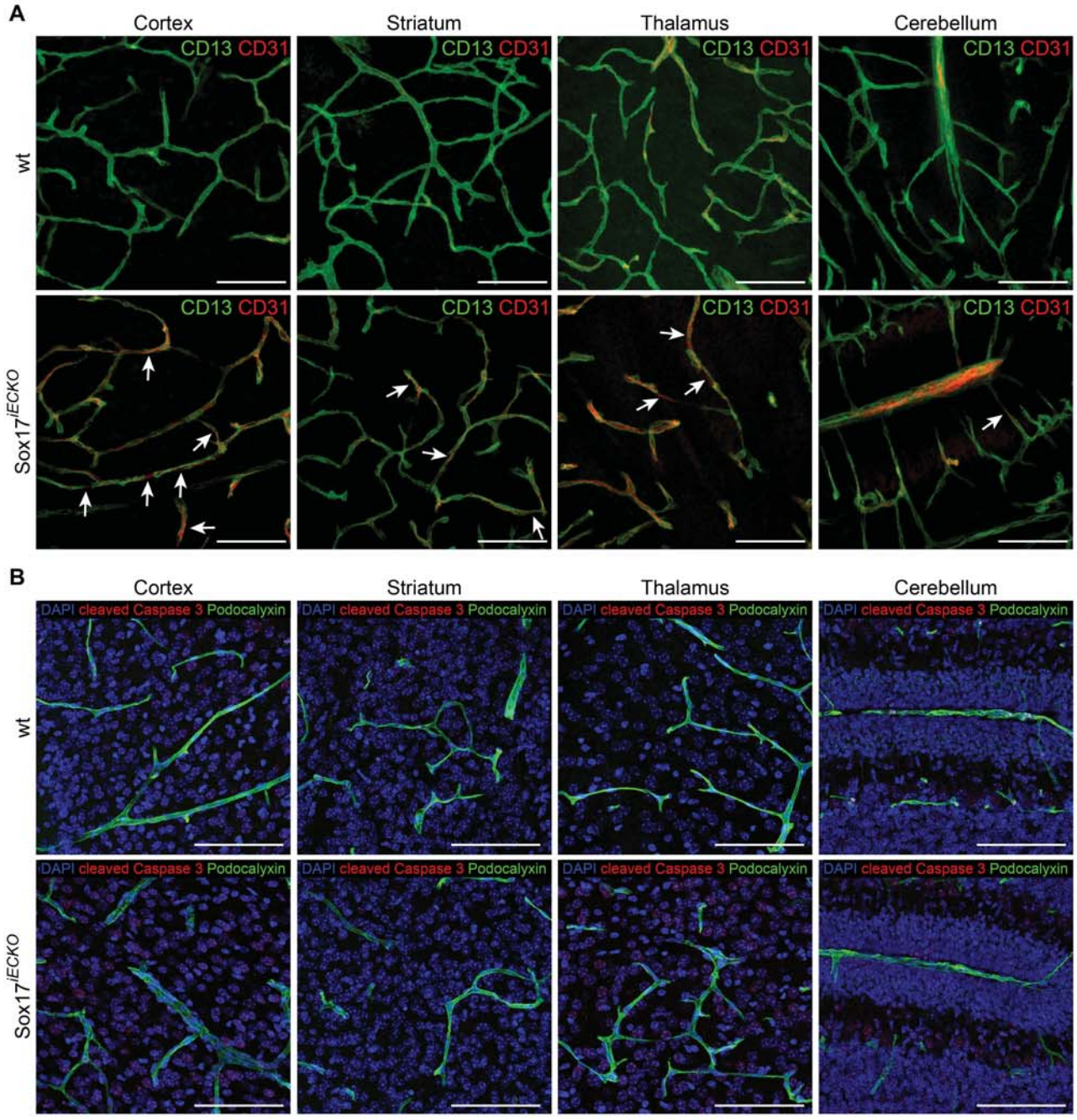

Online Figure IV. Endothelial Sox17 inactivation in post-natal pups

(A) Representative confocal images of the pericyte coverage (CD13 staining in green) and CD31(red) in different regions of wt and Sox17^{iECKO} pup brains. Vessels are labelled with CD31 (red) staining. Arrows point to vessel portions devoid of pericytes labeling. Scale bar: 100 μm.

(B) Representative confocal images of cleaved Caspase 3 (in red), in different regions of the brain, did not reveal any positive ECs neither in wt nor Sox17^{iECKO} pups. Vessels are labelled with Podocalyxin (green) staining while nuclei by DAPI (blue). Scale bar: 100 μm.

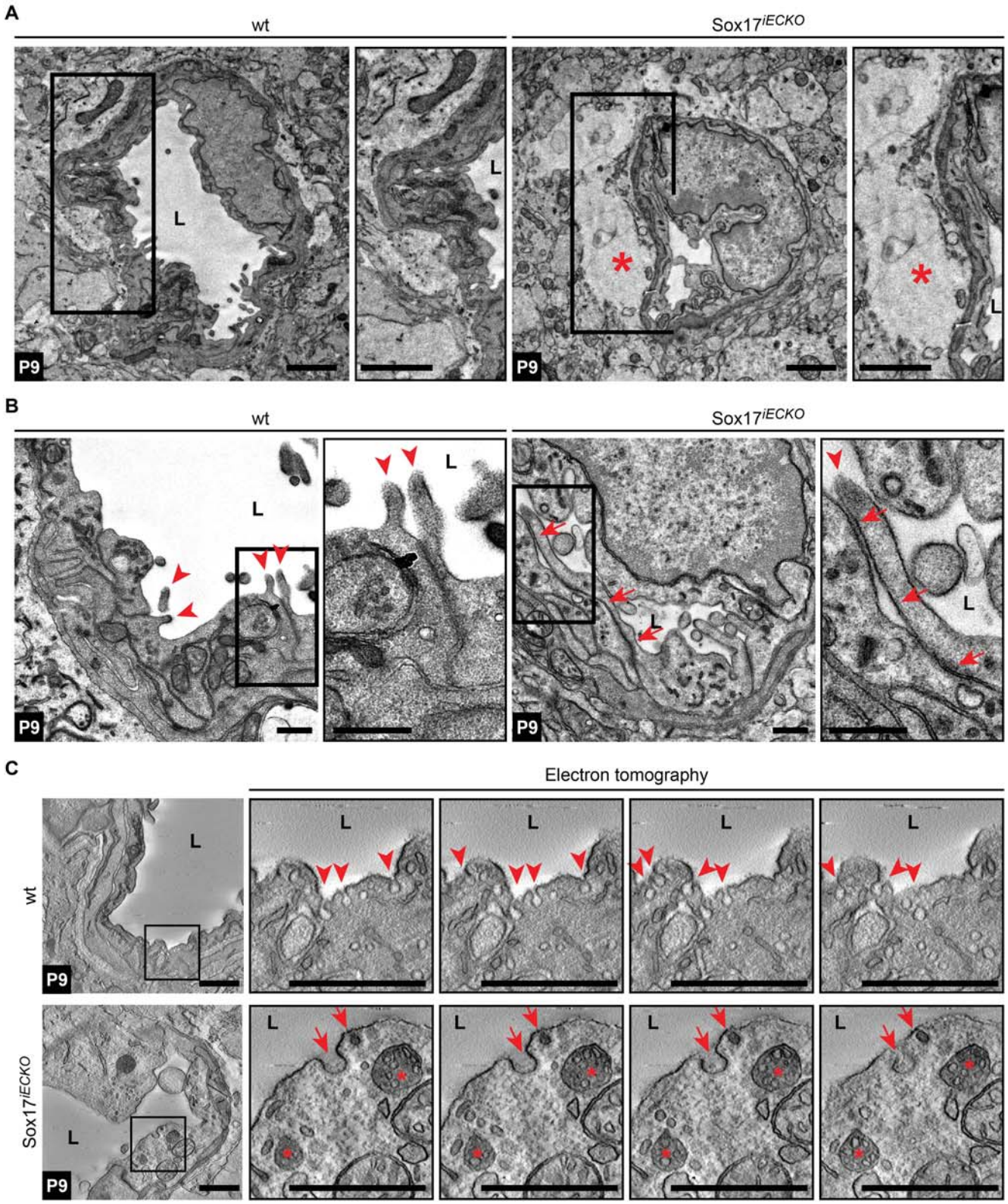

Online Figure V. Endothelial cells inactivation of Sox17 induces ultrastructural changes in post-natal pups brain microcirculation

(A) Edema (asterisk) in the interstitium near the capillary of Sox17*iECKO* mice (right panels) in comparison to the normal structure of the pericapillary space in wt mice (left panels). Scale bar: 2 μm. L means lumen.

(B) ECs of wt capillaris showed contacting cells extending intraluminal microvilli (arrowheads) into the vascular lumen. In contrast, overlapping (oblique) interendothelial contacts (arrows in right panels) were observed in the

capillary of the Sox17^{iECKO} mice. Scale bar: 500 nm. L means lumen.
(C) Electron tomography (four serial virtual images to the right are the enlargement boxed area in the left panels). Caveolae (red arrowheads) were observed in wt mice, but not in the Sox17^{iECKO} mice. Clathrin coated buds (arrows) and intracellular multivesicular bodies (asterisks) could be observed in Sox17^{iECKO} mice. Scale bar: L means lumen.

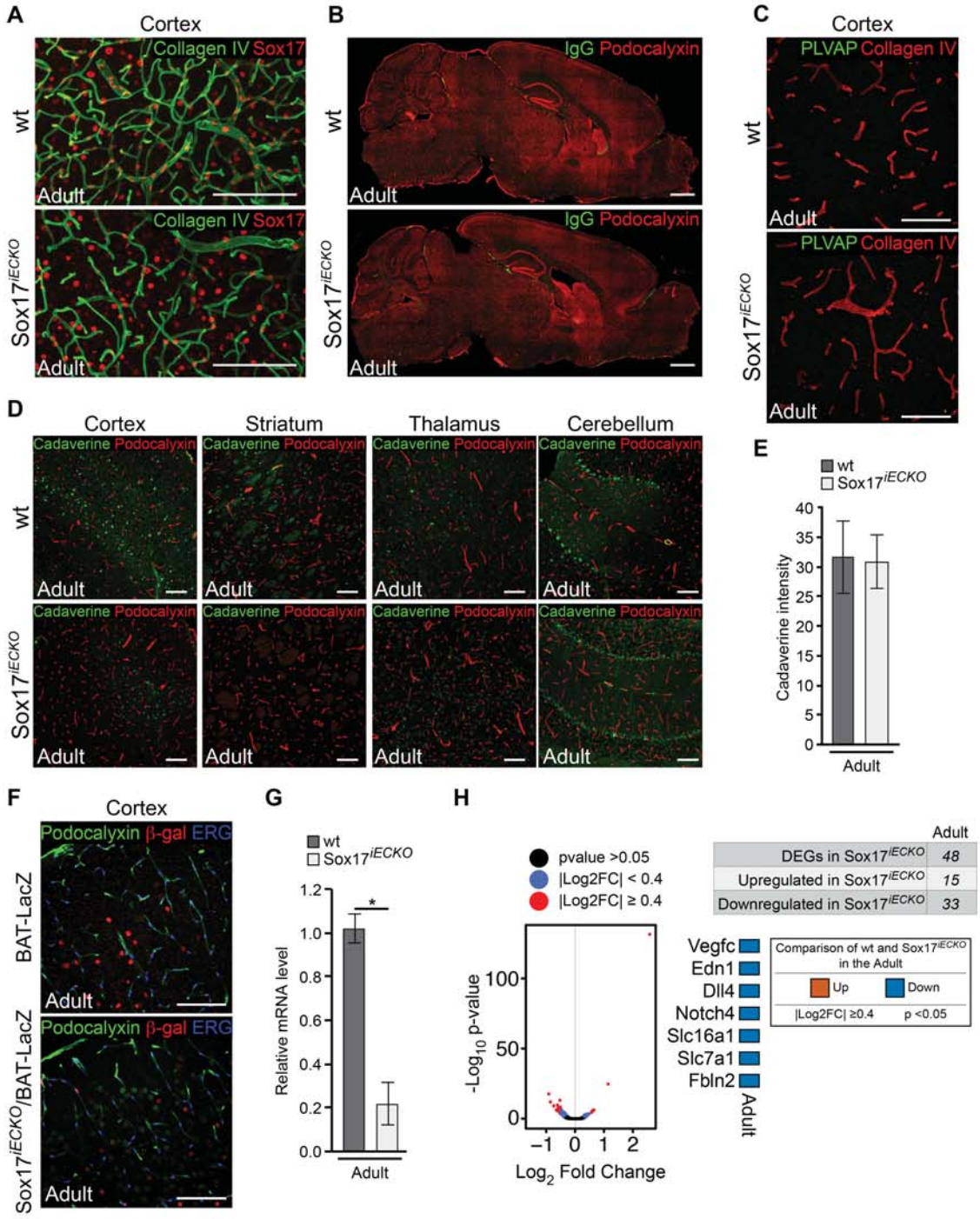

Online Figure VI. Endothelial Sox17 inactivation in brains of adult mice

(A-G) Confocal images of brain microvasculature. (A) Collagen IV (green) and Sox17 (red) staining in wt and Sox17^{iECKO} mice. Effective downregulation of Sox17 was observed in the brain vessels of Sox17^{iECKO} mice. Scale bar: 100 μm.

(B) IgG (green) and Podocalyxin (red) staining of vibratome sagittal sections. There is no detectable IgG leakage in the Sox17^{iECKO} brains. Scale bar: 1 mm.

(C) PLVAP (green) and Collagen IV (red) staining of brains (vibratome sections) of wt and Sox17^{iECKO} . Scale bar: 100 μm.

(D) Alexa555-conjugate Cadaverine (green) in vibratome brain sections from wt and Sox17^{iECKO} stained with Podocalyxin (red), and quantification of Cadaverin leakage (E), indicates no extravasation of the fluorescence tracer (n= 4 wt and 4 Sox17^{iECKO}). Scale bar: 100 μm.

(F) Cryosection of Sox17^{iECKO}/BAT-LacZ mutant. The number of β-gal positive nuclei (red) in the brain vessels, stained with podocalyxin (green), is already low in the wt, and there is no significant difference in the absence of Sox17, as also shown in Figure 7D. Scale bar: 100 μm.
(G) RT-qPCR analysis of *Sox17* expression in ECs isolated from brain microvasculature of wt and Sox17^{iECKO} mice and used for RNA-Seq (n= 4 wt and 4 Sox17^{iECKO} , * $p < 0.01$, two-tailed t-test assuming unequal variance).
(H) Differential gene expression between wt and Sox17^{iECKO} brain ECs. Volcano plots are used to display the magnitude (Log2 fold change) of the differential expression between wt and Sox17^{iECKO}. Each dot represents one gene that has detectable expression both in wt and Sox17^{iECKO} cells. Black dots represent genes that are not differentially expressed significantly (adjusted $p>0.05$). Significantly DEGs (adjusted $p\leq0.05$) are colored either in red ($|Log2FC|\geq0.4$) or in blue ($|Log2FC|<0.4$). The number of DEGs in Sox17^{iECKO} are reported in the table on top of the Volcano plots. Among the list of DEGs shown in Figure 6, up (orange) or down (blue) some relevant examples of the genes regulated in Sox17^{iECKO} are reported next to the Volcano plot.

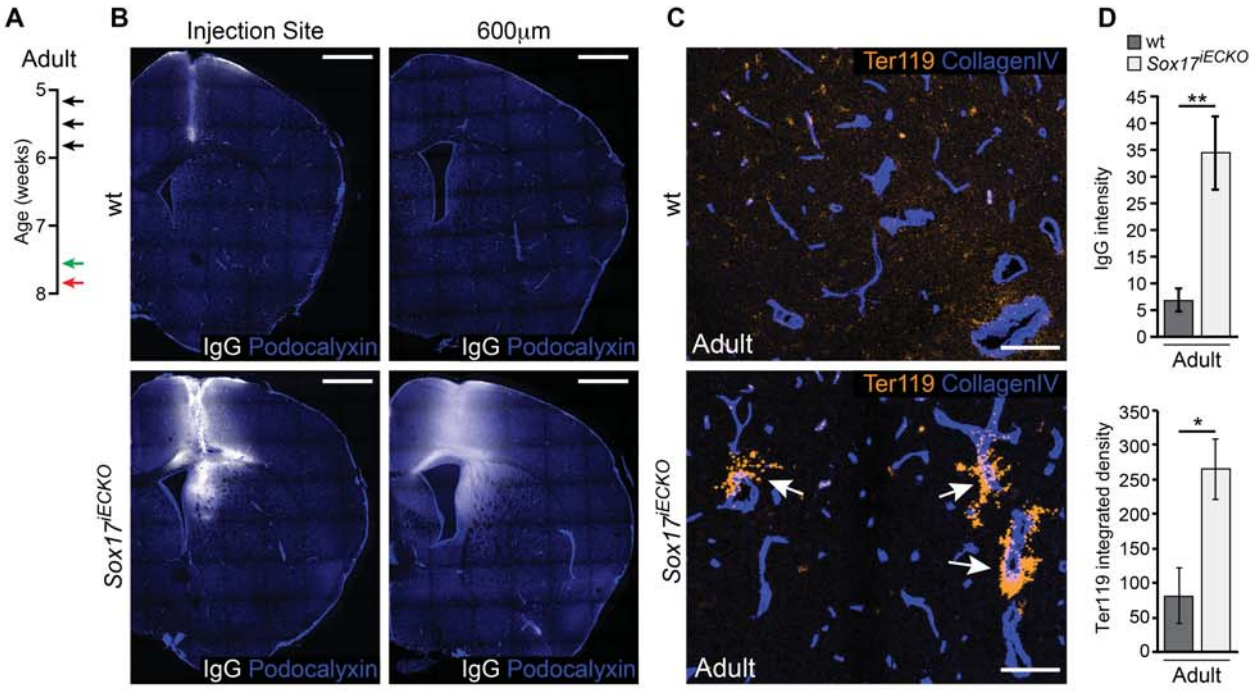

Online Figure VII. Sox17 deletion in ECs leads to higher vascular leakage with VEGF

(A) Diagram of Sox17 inactivation and analysis. Tamoxifen was injected in 5-week-old mice (three injections every other day; black arrows). Then, AAV-VEGF was injected transcranially to the frontoparietal cerebrum of mice (green arrow), and the brains were analysed 48 h after viral transduction (red arrow).

(B) Confocal analysis of brain vibratome sections at the injection site (left panels) and at a distal area (600 μm; right panels). Podocalyxin (blue) and IgG (white) staining revealed strong increases in IgG leakage in *Sox17*^{iECKO} mice. Vibratome sections were 100 μm thick. Scale bar: 1 mm.

(C) Confocal analysis of cryosections stained with Ter119 (orange) and collagen IV (blue). Hemorrhagic vessels (arrows) are seen only in *Sox17*^{iECKO} brains. Cryosections were 20 μm thick. Scale bar: 100 μm.

(D) Quantification of IgG leakage and hemorrhagic region in brains injected with AAV-VEGF. Data are represented as mean ± SD, *p <0.05; **p <0.01 (two-tailed t-test assuming unequal variance).

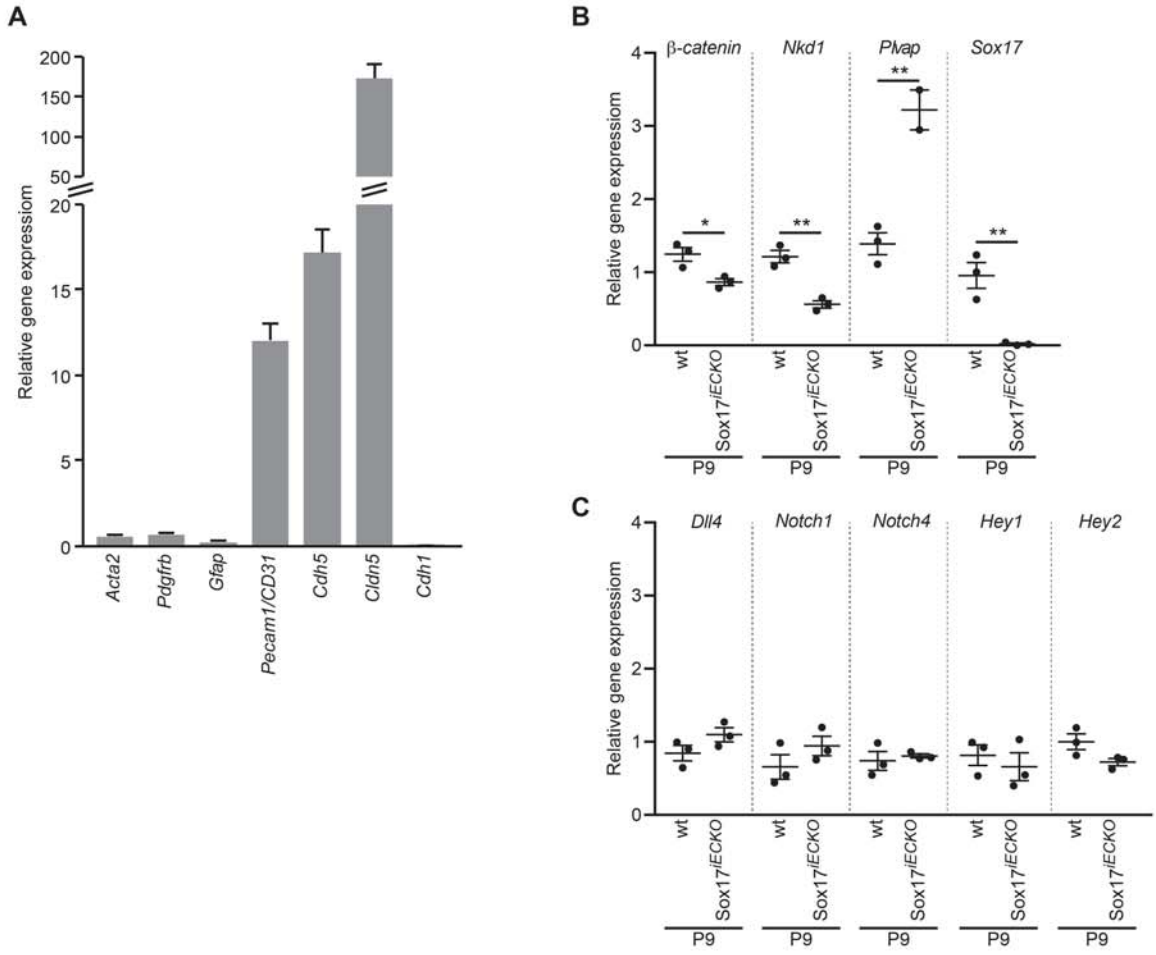

Online Figure VIII.

(A) RT-qPCR analysis of the transcript expressed by the ECs isolated from the brain microvasculature of wt adult mice and used for RNASeq. The expression levels of ECs-specific markers (*Pecam1*, *Cdh5*, *Cldn5*) compared to gene expressed by other cells of the NVU (as *Acta2*, *Pdgfrb*, *Gfap*, *Cdh1*) confirm strong enrichment of ECs-specific genes. Expression levels were normalized to *18S* using ΔCt method.

(B-C) RT-qPCR analysis of the transcript expressed by the ECs isolated from the brain microvasculature of wt and Sox17^{iECKO} pups and used for RNASeq. (B) Expression levels of β-*catenin*, *Nkd1* and *Sox17* were reduced in Sox17^{iECKO}, while *Plvap* expression level was increased. (C) The expression levels of Notch signaling pathway genes (*Dll4*, *Notch1*, *Notch4*, *Hey1 and Hey2*) were not affected by Sox17 deletion. Expression levels were normalized to *18S* using the ΔΔCt method (Sox17^{iECKO} *vs* wt) (n=3 wt and 3 Sox17^{iECKO}, * p <0.05 **p<0.01, Mann-Whitney test).

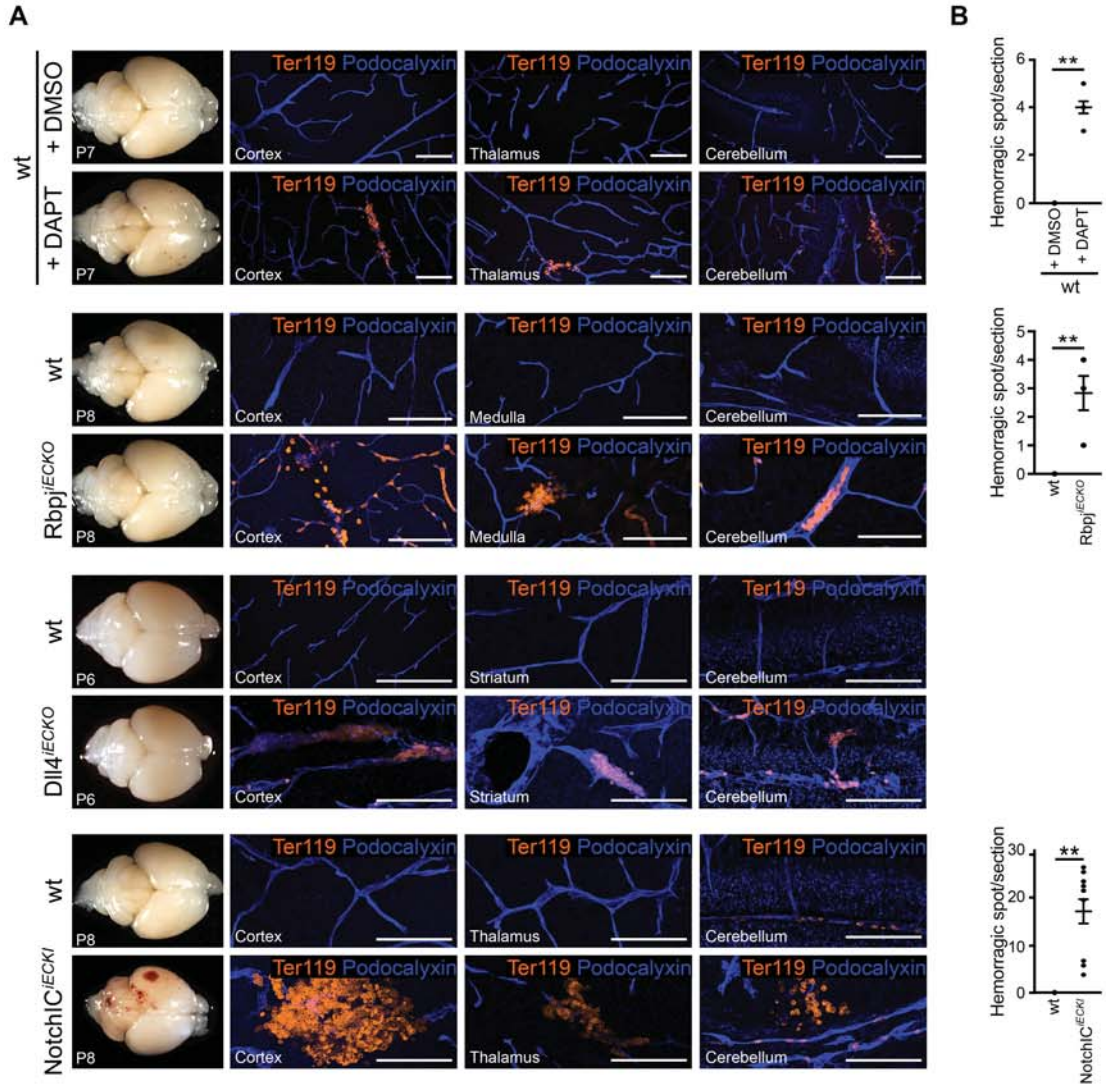

Online Figure IX. Notch signaling in the development of the brain microcirculation

(A) Representative overview (left) of whole brains and high magnification confocal images of Ter119 (erythrocytes marker, orange) and podocalyxin (blue) stained sections from control (right). Panels show, from top to bottom, DAPT treated (or DMSO as control), Rbpj^{iECKO}, Dll4^{iECKO} and NotchIC^{iECKI} and the corresponding control littermates. Note hemorrhages in DAPT treated, RBPJ^{iECKO} and NotchIC^{iECKI}. Rbpj^{iECKO} and Dll4^{iECKO} also shown enlarged vascular lumen.

(B) Count of hemorrhagic spot number per section of DAPT treated, Rbpj^{iECKO}, and NotchIC^{iECKI} (n=3 DMSO treated and 3 DAPT treated; n=3 wt and 3 Rbpj^{iECKO}; n=3 wt and 3 NotchIC^{iECKI}; **p<0.01, Mann-Whitney test).

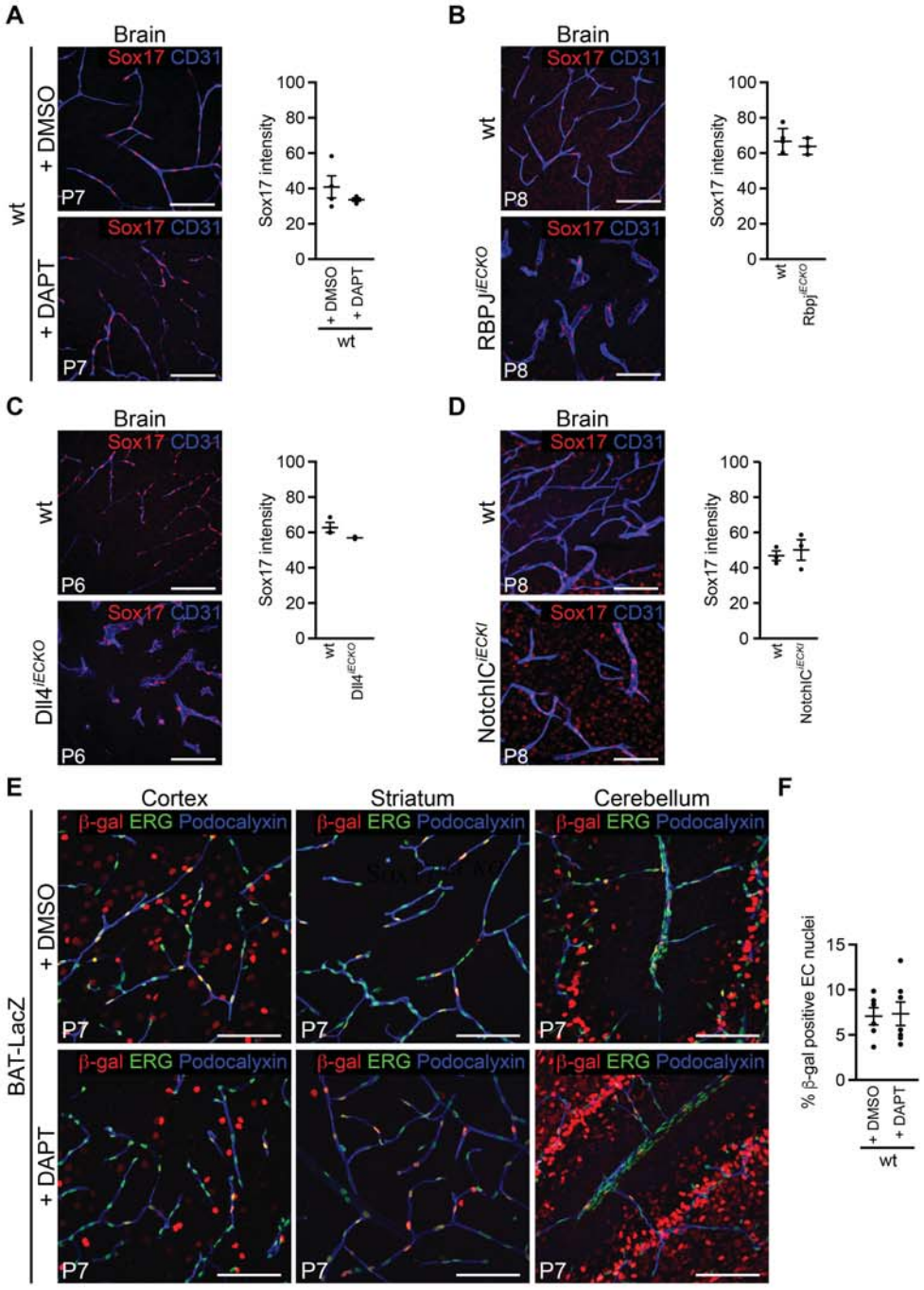

Online Figure X. Notch signaling does not influence Sox17 expression and β-catenin signaling

(A-D) Confocal images and the respective quantification (right) of Sox17 (red) expression in: DAPT treated (A), RPPJ*iECKO* (B), Dll4*iECKO* (C) and NotchIC*iECKI* (D). Vessels are labelled with CD31 (blue). Sox17 expression was not affected by Notch signaling modulation (n=4 DMSO treated and 5 DAPT treated; n=5 wt and 3 Rbpj*iECKO*; n=3 wt and 3 Dll4*iECKO*; n=3 wt and 3 NotchIC*iECKI*). Scale bar: 100 μm.

(E) Confocal analysis of vibratome sections of DAPT treated (or DMSO treated control) BAT-LacZ pups (see Methods for details). Brains sections were stained for ERG (green), β-gal (red) and Podocalyxin (blue). In the DAPT treated pups (lower panels), the number of β-gal positive ECs nuclei are not changed in all of the brain regions analyzed. Scale bar: 100 μm.

(F) Quantification of β-gal positive nuclei with respect of total ERG-positive ECs (percentages) as in (E). β-gal positive nuclei outside the vascular system indicate active Wnt signaling in the brain parenchyma.(n=7 DMSO treated and 7 DAPT treated).

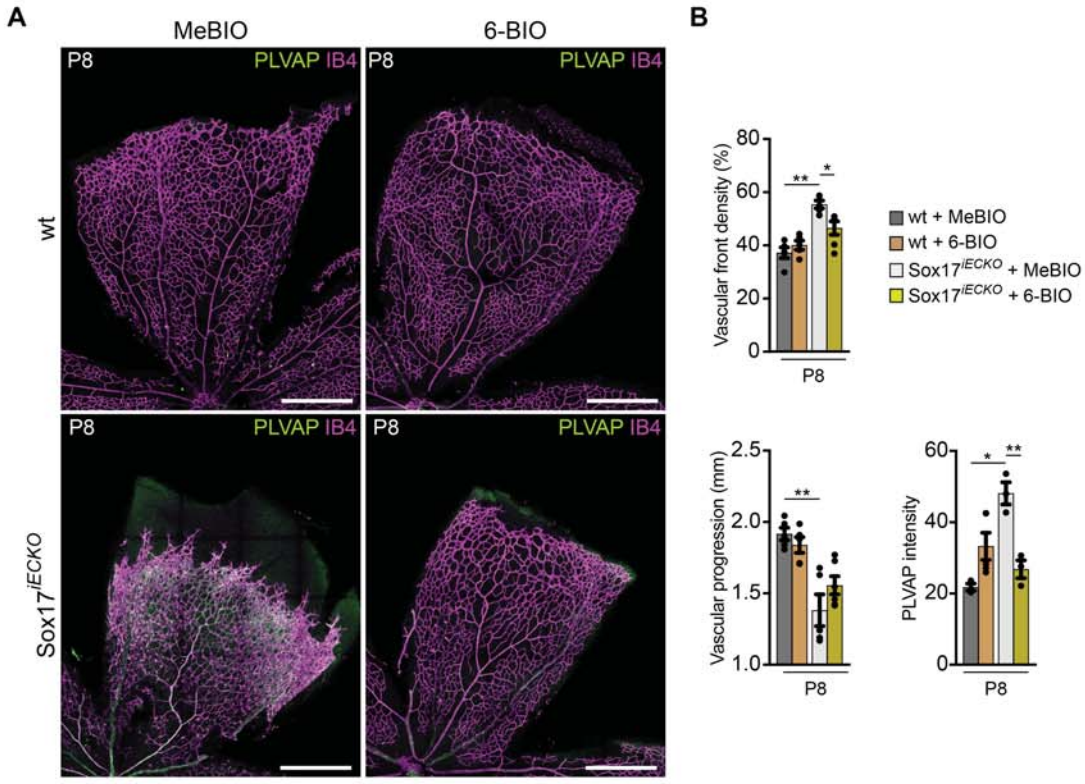

Online Figure XI. Stabilization of β-catenin signaling restores vascular defects induced by Sox17 inactivation

The experimental scheme of tamoxifen, 6-BIO or MEBIO injections is described in Figure 8.

(A) Confocal images of whole-mount retina stained with PLVAP (green) and isolectin B4 (IB4, in magenta) at P8, depicting almost complete rescue of the vascular phenotype of Sox17^{iECKO} treated with 6-BIO, as restored vascular front density and reduction in PLVAP expression compared to control (Me-BIO) treated animals. Scale bar: 500 μm.

(B) Quantification of vascular front density, vascular progression, PLVAP expression in the retina (n= 4 for each condition, *p <0.05 and **p <0.01, ANOVA followed by Tukey's post-hoc analysis). Data are represented as mean ± SEM.

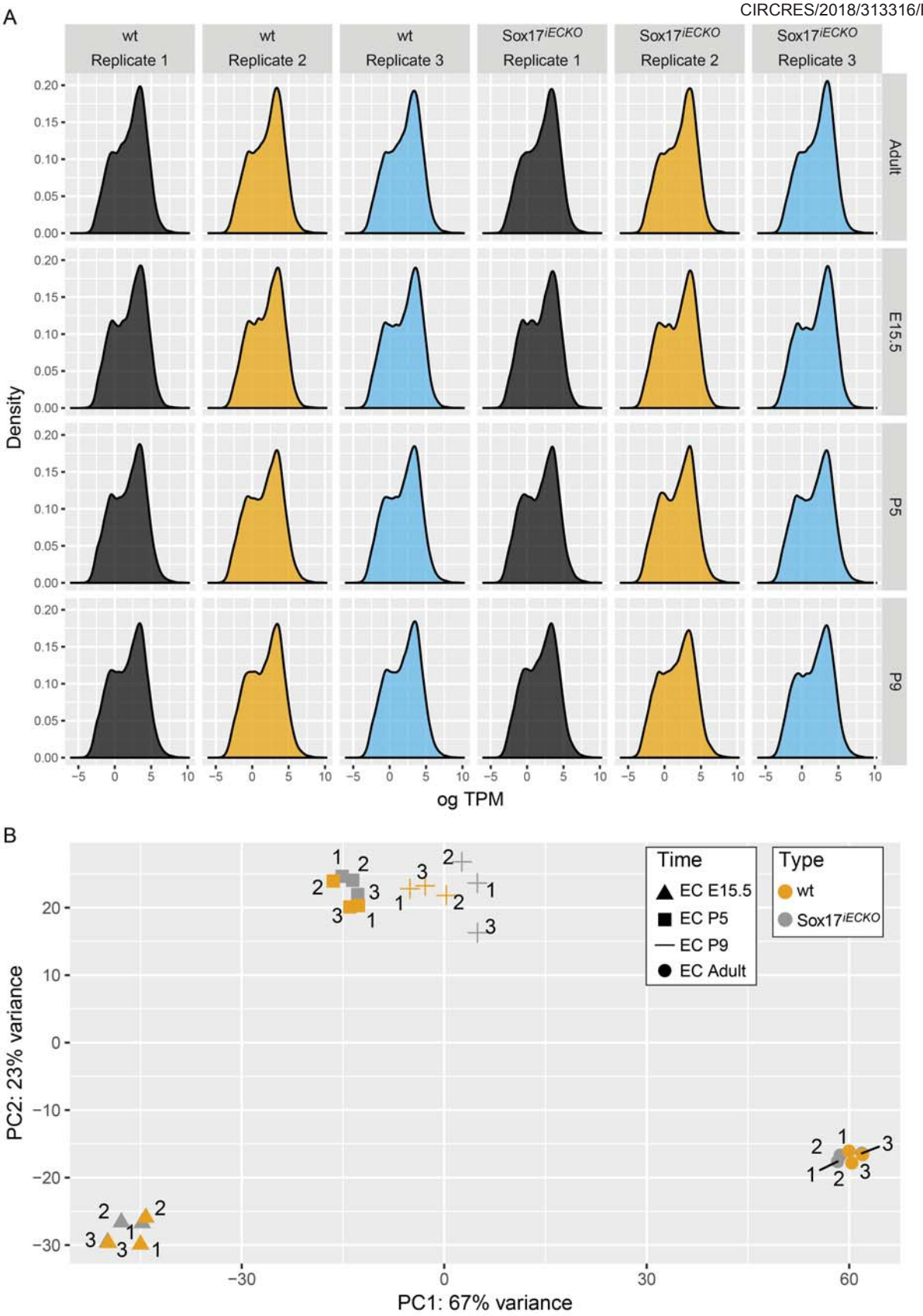

Online Figure XII Quality control of RNA-seq data.

(A) Distribution of gene expression levels. The gene expression level (log transformed TPM) follows a Poisson distribution in all samples and replicates.

(B) Principal component (PCA) plot of RNA-Seq data checking batch effect. The PCA plot is based on the normalized gene expression values obtained from DESeq2 using relative log expression normalization (RLE) method. It shows that the samples collected at the same time points are clustered together and the variability between biological replicates is low.

Online References

1. Kim I, Saunders TL, Morrison SJ. Sox17 dependence distinguishes the transcriptional regulation of fetal from adult hematopoietic stem cells. *Cell*. 2007;130:470-483
2. Harada N, Tamai Y, Ishikawa T, Sauer B, Takaku K, Oshima M, Taketo MM. Intestinal polyposis in mice with a dominant stable mutation of the beta-catenin gene. *EMBO J*. 1999;18:5931-5942
3. Maretto S, Cordenonsi M, Dupont S, Braghetta P, Broccoli V, Hassan AB, Volpin D, Bressan GM, Piccolo S. Mapping wnt/beta-catenin signaling during mouse development and in colorectal tumors. *Proc Natl Acad Sci U S A*. 2003;100:3299-3304
4. Koch U, Fiorini E, Benedito R, Besseyrias V, Schuster-Gossler K, Pierres M, Manley NR, Duarte A, Macdonald HR, Radtke F. Delta-like 4 is the essential, nonredundant ligand for notch1 during thymic t cell lineage commitment. *J Exp Med*. 2008;205:2515-2523
5. Han H, Tanigaki K, Yamamoto N, Kuroda K, Yoshimoto M, Nakahata T, Ikuta K, Honjo T. Inducible gene knockout of transcription factor recombination signal binding protein-j reveals its essential role in t versus b lineage decision. *Int Immunol*. 2002;14:637-645
6. Murtaugh LC, Stanger BZ, Kwan KM, Melton DA. Notch signaling controls multiple steps of pancreatic differentiation. *Proc Natl Acad Sci U S A*. 2003;100:14920-14925
7. Wang Y, Nakayama M, Pitulescu ME et al. Ephrin-b2 controls vegf-induced angiogenesis and lymphangiogenesis. *Nature*. 2010;465:483-486
8. Corada M, Nyqvist D, Orsenigo F, Caprini A, Giampietro C, Taketo MM, Iruela-Arispe ML, Adams RH, Dejana E. The wnt/beta-catenin pathway modulates vascular remodeling and specification by upregulating dll4/notch signaling. *Dev Cell*. 2010;18:938-949
9. Corada M, Orsenigo F, Morini MF, Pitulescu ME, Bhat G, Nyqvist D, Breviario F, Conti V, Briot A, Iruela-Arispe ML, Adams RH, Dejana E. Sox17 is indispensable for acquisition and maintenance of arterial identity. *Nat Commun*. 2013;4:2609
10. Vacik T, Lemke G. Dominant-negative isoforms of tcf/lef proteins in development and disease. *Cell Cycle*. 2011;10:4199-4200
11. Seibler J, Schubeler D, Fiering S, Groudine M, Bode J. DNA cassette exchange in es cells mediated by flp recombinase: An efficient strategy for repeated modification of tagged loci by marker-free constructs. *Biochemistry*. 1998;37:6229-6234
12. Bravi L, Rudini N, Cuttano R, Giampietro C, Maddaluno L, Ferrarini L, Adams RH, Corada M, Boulday G, Tournier-Lasserve E, Dejana E, Lampugnani MG. Sulindac metabolites decrease cerebrovascular malformations in ccm3-knockout mice. *Proc Natl Acad Sci U S A*. 2015;112:8421-8426
13. Fantin A, Vieira JM, Plein A, Maden CH, Ruhrberg C. The embryonic mouse hindbrain as a qualitative and quantitative model for studying the molecular and cellular mechanisms of angiogenesis. *Nat Protoc*. 2013;8:418-429
14. Gaal EI, Tammela T, Anisimov A, Marbacher S, Honkanen P, Zarkada G, Leppanen VM, Tatlisumak T, Hernesniemi J, Niemela M, Alitalo K. Comparison of vascular growth factors in the murine brain reveals placenta growth factor as prime candidate for cns revascularization. *Blood*. 2013;122:658-665
15. Bacigaluppi M, Pluchino S, Peruzzotti-Jametti L, Kilic E, Kilic U, Salani G, Brambilla E, West MJ, Comi G, Martino G, Hermann DM. Delayed post-ischaemic neuroprotection following systemic neural stem cell transplantation involves multiple mechanisms. *Brain*. 2009;132:2239-2251
16. Butti E, Bacigaluppi M, Rossi S et al. Subventricular zone neural progenitors protect striatal neurons from glutamatergic excitotoxicity. *Brain*. 2012;135:3320-3335
17. West MJ, Slomianka L, Gundersen HJ. Unbiased stereological estimation of the total number of neurons in thesubdivisions of the rat hippocampus using the optical fractionator. *Anat Rec*. 1991;231:482-497
18. Beznoussenko GV, Ragnini-Wilson A, Wilson C, Mironov AA. Three-dimensional and immune electron microscopic analysis of the secretory pathway in saccharomyces cerevisiae. *Histochem Cell Biol*. 2016;146:515-527
19. Mironov AA, Colanzi A, Polishchuk RS, Beznoussenko GV, Mironov AA, Jr., Fusella A, Di Tullio G, Silletta MG, Corda D, De Matteis MA, Luini A. Dicumarol, an inhibitor of adp-ribosylation of

ctbp3/bars, fragments golgi non-compact tubular zones and inhibits intra-golgi transport. *Eur J Cell Biol*. 2004;83:263-279
20. Kolpakov V, Polishchuk R, Bannykh S, Rekhter M, Solovjev P, Romanov Y, Tararak E, Antonov A, Mironov A. Atherosclerosis-prone branch regions in human aorta: Microarchitecture and cell composition of intima. *Atherosclerosis.* 1996;122:173-189
21. Bolte S, Cordelieres FP. A guided tour into subcellular colocalization analysis in light microscopy. *J Microsc*. 2006;224:213-232
22. Dobin A, Davis CA, Schlesinger F, Drenkow J, Zaleski C, Jha S, Batut P, Chaisson M, Gingeras TR. Star: Ultrafast universal rna-seq aligner. *Bioinformatics.* 2013;29:15-21
23. Anders S, Pyl PT, Huber W. Htseq--a python framework to work with high-throughput sequencing data. *Bioinformatics*. 2015;31:166-169
24. Durinck S, Moreau Y, Kasprzyk A, Davis S, De Moor B, Brazma A, Huber W. Biomart and bioconductor: A powerful link between biological databases and microarray data analysis. *Bioinformatics*. 2005;21:3439-3440
25. Nueda MJ, Tarazona S, Conesa A. Next masigpro: Updating masigpro bioconductor package for rna-seq time series. *Bioinformatics*. 2014;30:2598-2602
26. Love MI, Huber W, Anders S. Moderated estimation of fold change and dispersion for rna-seq data with deseq2. *Genome Biol.* 2014;15:550
27. Alexa A, Rahnenfuhrer J. Topgo. 2017
28. Balconi G, Spagnuolo R, Dejana E. Development of endothelial cell lines from embryonic stem cells: A tool for studying genetically manipulated endothelial cells in vitro. *Arterioscler Thromb Vasc Biol.* 2000;20:1443-1451
29. Liebner S, Corada M, Bangsow T et al. Wnt/beta-catenin signaling controls development of the blood-brain barrier. *J Cell Biol.* 2008;183:409-417
30. Francois M, Caprini A, Hosking B et al. Sox18 induces development of the lymphatic vasculature in mice. *Nature*. 2008;456:643-647